

OPTICAL FIBRES

PACS numbers: 42.81.Bm; 42.81.Dp; 42.70.Qs
DOI: 10.1070/QE2012v042n02ABEH014736

Silica-core photonic bandgap fibres: Properties and a criterion for single-mode operation

O.N. Egorova, S.L. Semjonov, M.Yu. Salganskii, V.F. Khopin, A.N. Gur'yanov

Abstract. **We have studied the properties of silica-core photonic bandgap fibres with a small diameter to pitch ratio (no greater than 0.4) of high-index rods and small refractive-index difference (no greater than 0.03) in the cladding. Theoretical analysis and experimental data demonstrate that the number of core modes depends only on the number of pure-silica elements that form the core and is independent of cladding parameters. If there is one such element, only one dispersion curve of a core mode falls in the fundamental bandgap and the fibre is single-mode. The fibres having seven such elements are multimode.**

Keywords: *photonic bandgap fibres, large mode field diameter fibres.*

1. Introduction

One problem confronting designers of fibre laser systems with high beam intensity in the fibre core and considerable fibre length is undesirable nonlinear optical effects, which limit the power and energy of pulses capable of propagating through the fibre without distortions. The beam intensity in the fibre core can be reduced by increasing its diameter. One of the most successful large core diameter fibre designs so far is that having a silica core and a holey microstructured cladding with a small hole diameter to pitch ratio [1].

One advantage of the fibre designs with a holey microstructured cladding is that they offer the possibility of 'endlessly single-mode' operation, i.e., single-mode operation in a wide spectral region, because the difference between the refractive index of the core and the effective refractive index of the cladding decreases considerably with decreasing wavelength [2, 3]. Unfortunately, such fibres have a number of drawbacks, including the presence of holes, which may accumulate contaminants capable of markedly reducing the reliability and optical damage threshold of the fibre. To eliminate this drawback, an extra step after the fibre fabrication process is needed that would allow the holes to be stopped up at the fibre ends, without impairing the guidance properties of the fibre. Another problem is that the fibre drawing process becomes significantly more complicated: the hole diameter may vary widely depending on the pressure in the holes. This makes drawing results less predictable because of the high probability that the cross-sectional fibre structure will be distorted.

An alternative solution is silica-core fibres having a microstructured reflective cladding without holes. The guided light is here confined to the core through photonic bandgap effects [4, 5]. Such fibres have been proposed comparatively recently and their optical properties have not yet been studied in sufficient detail.

An all-solid photonic bandgap fibre is a two-dimensional photonic crystal with a solid core formed by one or more elements containing no doped regions. As an example, Fig. 1 shows the cross sections of two such fibres. The cladding of the fibres contains an array of rods of diameter d. The rods are parallel to the fibre axis and their refractive index is a few percent above that of undoped silica glass. The centre-to-centre spacing between the rods (pitch) is Λ. The core mode is excited at wavelengths that fall within the photonic bandgaps

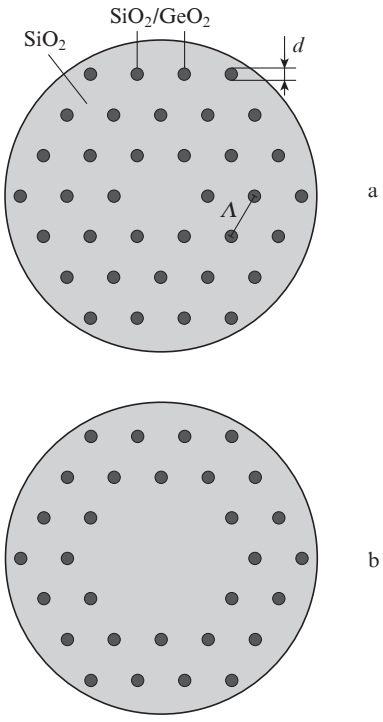

Figure 1. Cross sections of photonic bandgap fibres with a silica core formed by (a) one and (b) seven elements containing no doped regions.

O.N. Egorova, S.L. Semjonov Fiber Optics Research Center, Russian Academy of Sciences, ul. Vavilova 38, 119333 Moscow, Russia; e-mail: egorova@fo.gpi.ru, sls@fo.gpi.ru;
M.Yu. Salganskii, V.F. Khopin, A.N. Gur'yanov G.G. Devyatykh Institute of Chemistry of High-Purity Substances, Russian Academy of Sciences, ul. Tropinina 49, 603950 Nizhnii Novgorod, Russia; e-mail: misalgan@yandex.ru

Received 4 October 2011; revision received 26 December 2011
Kvantovaya Elektronika **42** (2) 165–169 (2012)
Translated by O.M. Tsarev

of the cladding. Photonic bandgap fibres have no air holes and are thus easier to fabricate and employ in comparison with holey fibres.

Egorova et al. [5] were the first to study a photonic bandgap fibre with a rod diameter to pitch ratio $d/\Lambda < 0.4$. The low value of this ratio allowed Λ to be increased, which in turn offered the possibility of increasing the mode field diameter to 20 μm. The bandgap was several hundred nanometres in width, and the optical loss level was quite acceptable. It is also worth noting that, at a small d/Λ ratio, efficient end pumping of such fibres is possible because the fraction of the pump light captured by the rods will be proportional to $(d/\Lambda)^2$. At high d/Λ ratios, this fraction will be rather large, whereas for $d/\Lambda < 0.2$ the pump power loss will be as low as a few percent.

The ability to further increase the mode field diameter in photonic bandgap fibres, while maintaining single-mode waveguiding, depends crucially on knowledge of how the key parameters of the fibre cladding and core influence the mode composition of the fibre. This issue is addressed in this paper.

2. Numerical modelling

The dispersion characteristics of cladding and core modes were computed in a planewave basis [6] using the MIT Photonics-Bands (MPB) package [7].

The band diagram of cladding modes at a refractive-index difference between the rods and undoped silica matrix $\Delta n = 0.015$ and $d/\Lambda = 0.1$ is presented in Fig. 2, with $(\beta - kn_0)\Lambda$ and λ/Λ axes, where β is the mode propagation constant; $k = 2\pi/\lambda$; and n_0 is the refractive index of undoped silica glass. Cladding modes exist in the grey areas, and bandgaps are located below the silica glass 'level', $(\beta - kn_0)\Lambda = 0$ (white areas). Figure 2 shows three bandgaps: I–III. Bandgap I (the fundamental bandgap of the photonic crystal cladding) is located in the longest wavelength region. The lower and upper boundaries of bandgap I (β_L and β_U, respectively) intersect the silica glass level at points *1* and *2*.

The dispersion curve of the core mode lies between the bandgap boundaries β_L and β_U. Therefore, the propagation constant of the core mode, β, meets the relations $\beta_L < \beta < kn_0$ in region *1–2* and $\beta_L < \beta < \beta_U$ in region *2–3*. Since a mode with a propagation constant β is inclined at $\theta = \arccos[\beta/(kn_0)]$ to the fibre axis, the bandgap boundaries determine the maximum and minimum mode propagation angles, i.e. the numerical aperture of the fibre: NA = $n_0 \sin\theta$.

Core mode cutoff occurs when the dispersion curve intersects the lower or upper bandgap boundary at point *a* or *b*, respectively. Each core mode has both a shorter (point *a*) and a longer (point *b*) cutoff wavelength.

Thus, the bandgap boundaries determine the spectral range where the core mode exists and the maximum and minimum mode propagation angles.

To understand how the parameters of the photonic crystal cladding influence the position of the boundaries of the fundamental bandgap, we calculated band diagrams for three values of Δn (0.005, 0.015 and 0.030) and five values of d/Λ (0.05, 0.1, 0.2, 0.3 and 0.4).

Hereafter, we use the relative bandgap $\Delta\lambda/\lambda_m = (\lambda_3 - \lambda_1)/\lambda_m$, where λ_1 and λ_3 are the wavelengths corresponding to points *1* and *3* (Fig. 2), and $\lambda_m = (\lambda_3 + \lambda_1)/2$ can be taken as the midgap wavelength. It is worth pointing out that $\Delta\lambda/\lambda_m$ characterises only the bandgap, and the region in which the core mode is confined is narrower and is defined by the points where the dispersion curve of the mode (or modes in the case of multimode fibre) intersects the bandgap edges.

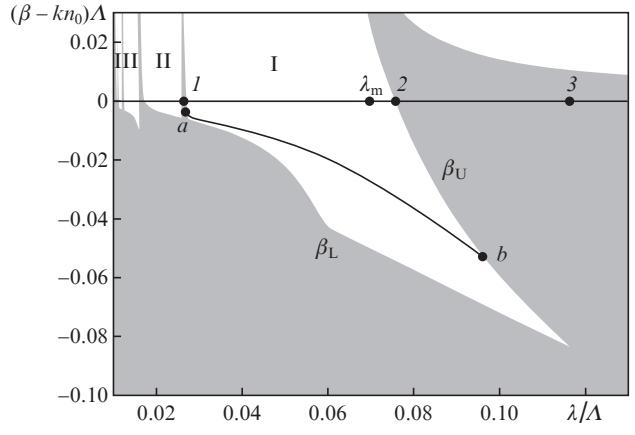

Figure 2. Band diagram of a fibre with a refractive-index difference in the cladding $\Delta n = 0.015$ and $d/\Lambda = 0.1$. The fibre core is formed by one pure-silica element. Cladding modes can exist in the grey areas, and bandgaps are located in the white areas; curve *ab* represents the dispersion relation of the core mode; $\lambda_m = (\lambda_3 + \lambda_1)/2$.

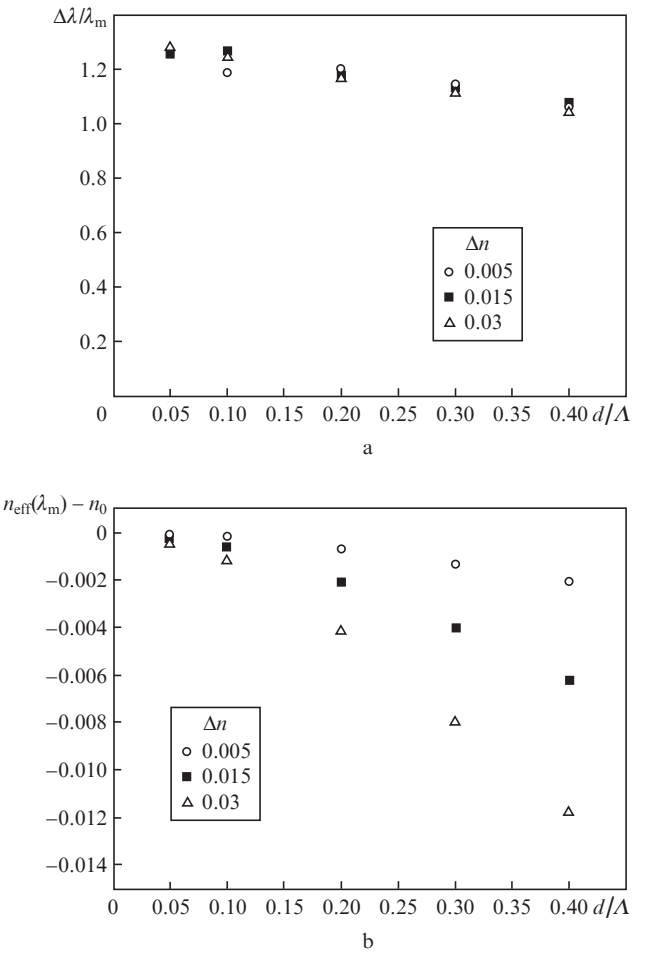

Figure 3. (a) Relative bandgap and (b) midgap core–cladding index contrast at different Δn values.

Figure 3a shows the relative bandgap $\Delta\lambda/\lambda_m$ as a function of d/Λ at different values of Δn in the cladding. As seen, $\Delta\lambda/\lambda_m$ is independent of Δn and increases, albeit only slightly, with decreasing d/Λ. At the same time, the difference between the refractive index of the core and the effective refractive index of the cladding at the midgap wavelength increases considerably in magnitude with an increase in both d/Λ and Δn (Fig. 3b).

To assess the mode composition of the fibres with a core formed by one or seven pure-silica elements, we examined calculated dispersion curves lying in the fundamental bandgap. Calculations were made for $\Delta n = 0.005$, 0.015 and 0.03 and $d/\Lambda = 0.05$, 0.1, 0.2, 0.3 and 0.4. The results for $\Delta n = 0.015$ and $d/\Lambda = 0.1$ are presented in Figs 2 (one pure-silica element) and 4 (seven pure-silica elements). For the other combinations of the parameters, the core has the same mode composition and similar dispersion diagrams.

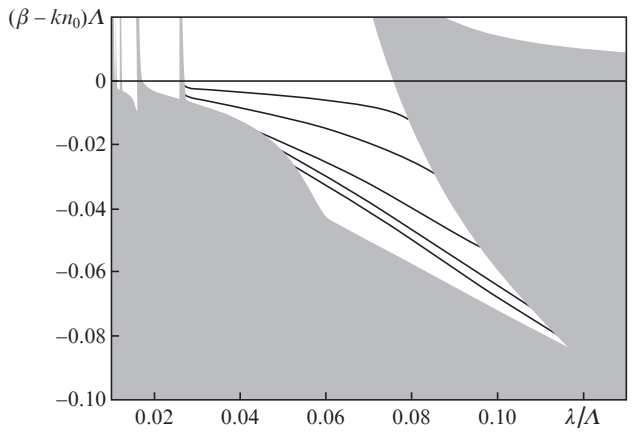

Figure 4. Band diagram of a fibre with a core formed by seven pure-silica elements; $\Delta n = 0.015$, $d/\Lambda = 0.1$.

As seen in Fig. 2, only one (doubly degenerate) core mode falls within the fundamental bandgap. Thus, the fibres having one pure-silica element are single-mode throughout the fundamental bandgap. In the case of the fibres having seven pure-silica elements, the dispersion relations of 14 modes fall in the bandgap. Because some of these are degenerate, they form five groups of modes similar in dispersion curve. The mode composition obtained is similar to that reported by Guobin et al. [8] for holey microstructured fibres.

3. Experimental procedure and results

The above results were verified experimentally using several fibres with a core formed by one or seven pure-silica elements. The fibres were fabricated by the stack-and-draw technique. Microstructured fibre preforms were produced by stacking individual cylindrical elements, each serving as a preform for an element of the fibre cladding or core. The assembly was sintered into a monolithic preform, which was then drawn into fibre. The preform elements for the cladding were produced by drawing MCVD preforms with a germania-doped core, and those for the core were drawn from a cylindrical undoped silica preform. Table 1 lists the key parameters of the fibres, and Fig. 5 shows scanning electron micrographs of their cross sections.

The mode composition of the fibres was studied by observing the output near-field intensity distribution under various

Table 1. Parameters of the photonic crystal fibres.

Fibre no.	d/Λ	Λ/μm	Δn	Pure-silica elements	Layers in the cladding	Mode composition
1	0.24	9.2	0.0185	7	6	Multimode
2	0.08	18	0.028	7	2	Multimode
3	0.12	11.4	0.028	1	6	Single-mode
4	0.09	28.8	0.005	1	3	Single-mode

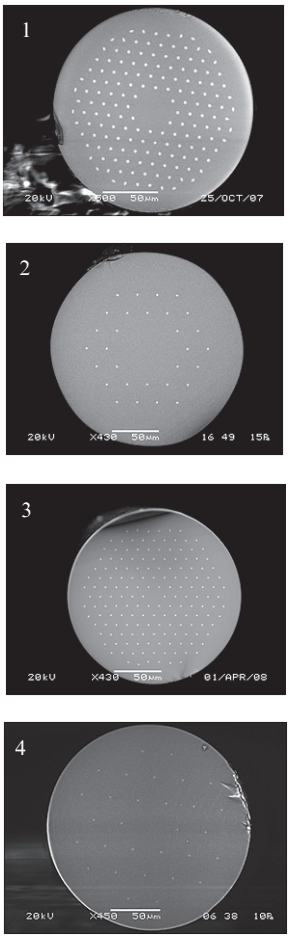

Figure 5. Scanning electron micrographs of the end faces of fibres 1–4 (Table 1).

excitation conditions using a CCD camera. Light from an external source was launched into the fibre under test through an input fibre butt-coupled to the test fibre. Displacing the end face of the input fibre, we varied the mode excitation conditions in the test fibre.

Under any excitation conditions, the fibres with a core formed by one pure-silica element had a Gaussian output intensity distribution, which corresponded to the fundamental mode. In the fibres with a core formed by seven pure-silica elements, the output intensity distribution depended on excitation conditions, suggesting that these fibres were multimode. Thus, the fibres having one pure-silica element were single-mode and those having seven such elements were multimode, in agreement with the calculation results above.

In the case of a core formed by several pure-silica elements, the number of core modes increases with mode field diameter, making it difficult to produce a high-quality beam of fibre lasers and amplifiers. When the core is formed by one pure-

silica element, the mode field diameter can be increased by increasing the spacing between the rods in the cladding. Fibre 4 (Fig. 5) has the largest spacing between the rods in the photonic crystal cladding, $\Lambda = 28.8$ μm, which is about 30 times the working wavelength, and its core is formed by one pure-silica element. The other parameters of fibre 4 are such that the centre wavelength of its fundamental bandgap is 1 μm: $d/\Lambda = 0.09$ and $\Delta n = 0.005$. The number of layers in its cladding is three because, in a real cladding-pumped laser, the pump region diameter should be relatively small (200–300 μm). In the case of the three-layer photonic crystal cladding, the fibre diameter (pump region diameter) is 200 μm.

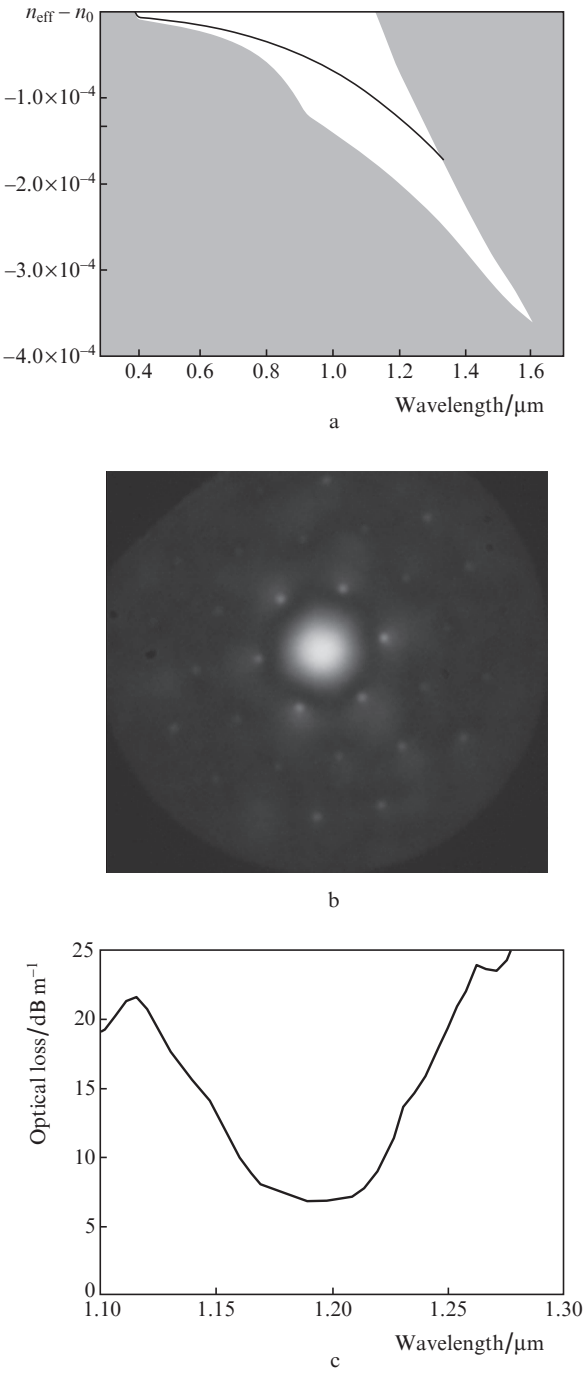

Figure 6. (a) Band diagram of fibre 4 (Table 1), (b) power distribution across its output end and (c) its optical loss spectrum.

The band diagram of fibre 4 is presented in Fig. 6a. The numerical aperture at the midgap wavelength of this fibre is 0.025, which corresponds to a core–cladding index difference of about 2×10^{-4}. The points where the dispersion curve of the core mode intersects the bandgap edges correspond to wavelengths of 400 and 1300 nm. In the range 400–700 nm, the dispersion curve of the mode is close to one of the bandgap edges.

The near-field power distribution at the output end of fibre 4 (of 10-cm length) was recorded using a CCD camera (Fig. 6b). Stable mode confinement occurred in the range 800–1200 nm (the longer wavelength limit was set by the working range of the CCD camera). Fibre 4 had a Gaussian output power distribution under various excitation conditions, indicating that the fibre was single-mode. The mode field diameter at 1050 nm was 35 μm as measured with the CCD camera. The optical loss in a straight piece of the fibre was measured by the cut-back technique and was found to be 6 dB m^{-1} in the range 1–1.2 μm (Fig. 6c). The reason for the high optical loss level is that the wings of the transverse mode field distribution penetrate beyond the photonic crystal cladding and the mode becomes leaky. Thus, increasing the core diameter through an increase in the spacing between the rods in the cladding leads to a rise in optical loss level.

4. Conclusions

We have studied the mode composition of silica-core photonic bandgap fibres having a small rod diameter (d) to spacing (Λ) ratio ($d/\Lambda \leqslant 0.4$) and small refractive-index difference in the cladding ($\Delta n = 0.005–0.03$).

Our calculations demonstrate that the number of core modes in the fundamental bandgap in the range of parameters studied depends only on the number of pure-silica elements in the core. If there is one such element, only one core mode (doubly degenerate with respect to its polarisation) falls in the fundamental bandgap. The fibres having seven such elements are multimode. The mode composition of the core is independent of the cladding parameters Δn and d/Λ. The modelling results agree with experimental data.

The mode field diameter in such fibres can be increased by increasing the number of pure-silica elements in the core or the spacing between the rods in the cladding. Both approaches, however, have inherent drawbacks.

Increasing the mode field diameter through an increase in the number of pure-silica elements in the core from one to seven leads to multimode operation, which requires further design modifications in order to strip higher order modes and makes it difficult to reach high laser beam quality.

Increasing the mode field diameter through an increase in the spacing between the rods in the photonic crystal cladding allows single-mode behaviour to be retained but leads to an increase in optical loss. The mode becomes leaky because the wings of the transverse mode field distribution penetrate beyond the cladding. For example, in a fibre with $\Lambda = 28.8$ μm, $d/\Lambda = 0.09$, $\Delta n = 0.005$ and a core formed by one pure-silica element, the mode field diameter was 35 μm and the optical loss was 6 dB m^{-1}.

Similar problems are encountered in the case of microstructured (holey) fibres, so studies aimed at improving the performance of the two types of fibres are of great current interest.

Acknowledgements. We are grateful to E.M. Dianov for initiating and supporting our work. This research was sponsored

by the RF President's Grants Council (Support to Young Russian Scientists Programme, Grant No. MK-8069.2010.2) and the Russian Foundation for Basic Research (Grant No. 10-02-00334-a).

References

1. Knight J.C., Birks T.A., Russell P.St.J., Atkin D.M. *Opt. Lett.*, **21**, 1547 (1996).
2. Birks T.A., Knight J.C., Russell P.St.J. *Opt. Lett.*, **22**, 961 (1997).
3. Joannopoulos J.D., Johnson S.G., Winn J.N., Meade R.D. *Photonic Crystals. Molding the Flow of Light* (Princeton and Oxford: Princeton University Press, 2008).
4. Argyros A., Birks T.A., Leon-Saval S.G., Cordeiro C.M.B., Luan F., Russell P.St.J. *Opt. Express*, **13**, 309 (2005).
5. Egorova O.N., Semjonov S.L., Kosolapov A.F., Denisov A.N., Pryamikov A.D., Gaponov D.A., Biriukov A.S., Dianov E.M., Salganskii M.Y., Khopin V.F., Yashkov M.V., Gurianov A.N., Kuksenkov D.V. *Opt. Express*, **16**, 11735 (2008).
6. Johnson G.S., Joannopoulos J.D. *Opt. Express*, **8**, 173 (2001).
7. ab-initio.mit.edu/mpb
8. Guobin R., Zhi W., Shuqin L., Shuisheng J. *Opt. Express*, **11**, 1310 (2003).